Journal of Porphyrins and Phthalocyanines
J. Porphyrins Phthalocyanines 2025; **29**: A–H
DOI: 10.1142/S1088424625500622
(pp. 8)

Published at https://www.worldscinet.com/jpp/

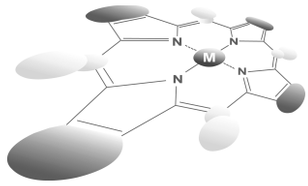

Silicon phthalocyanines with tetraphenylethene substituents: Synthesis, photophysical and aggregation-induced emission properties

Yolande Ikala Openda, Martín Guarini-Román, Luis Martín-Gomis and Ángela Sastre-Santos*

Área de Química Orgánica, Instituto de Bioingeniería, Universidad Miguel Hernández, Avda. Universidad S/N, 03202, Elche, Spain

Received 31 March 2025
Accepted 29 April 2025

Dedicated to Prof. Karl M. Kadish on the occasion of his 80th birthday

ABSTRACT: This work presents the synthesis and characterization of three silicon phthalocyanine derivatives, SiPc **1**, SiPc **2** and SiPc **3**, incorporating tetraphenylethylene (TPE) units at peripheral and axial positions, to evaluate their photophysical properties and aggregation-induced emission (AIE) behavior. SiPc **1**, axially substituted with TPE, exhibited diminished fluorescence and singlet oxygen generation, but displayed AIE in the near-infrared region (700–900 nm) upon water addition. SiPc **2**, with peripheral TPE units, showed enhanced fluorescence and singlet oxygen generation without AIE. SiPc 3, featuring axial and peripheral TPE units, demonstrated reduced fluorescence, singlet oxygen generation, and no AIE. These results highlight the ability to modulate photodynamic activity and AIE properties through strategic TPE substitution on silicon phthalocyanines, suggesting potential applications in image-guided phototherapy.

KEYWORDS: silicon phthalocyanines, tetraphenylethene, aggregation-induced emission, singlet oxygen generation, photodynamic therapy

INTRODUCTION

Phthalocyanines, synthetic analogs of porphyrins, are recognized for their diverse applications in technology and biomedicine. This versatility arises from their capacity for structural modification, achieved through variations in the central metal and peripheral, non-peripheral, and axial substituents [1, 2]. Specifically, axially substituted silicon phthalocyanine (SiPc) derivatives have emerged as second-generation photosensitizers for photodynamic therapy (PDT) [3] in cancer and non-cancer pathologies [4–6]. Their efficacy is attributed to strong absorption in the red, far red and near infrared regions (Q-band, ~650–800 nm), facilitating deep tissue penetration, and efficient singlet oxygen generation upon photoactivation. This singlet oxygen triggers the photodynamic process, inducing the generation of reactive oxygen species (ROS) near malignant cells, thereby killing them and minimizing systemic toxicity. However, the clinical application of SiPcs is limited by their inherent hydrophobicity and tendency to aggregate in aqueous environments. This leads to aggregation-caused quenching (ACQ) of fluorescence and reduced ROS generation. This limitation could prevent their application in biological systems. Conventional molecular design strategies have focused on enhancing hydrophilicity by incorporating solubilizing substituents [7]. An alternative approach to overcome the ACQ effect involves integrating fluorescent functional groups that exhibit aggregation-induced emission (AIE). AIE describes the phenomenon observed in specific molecules, known as AIEgens, which exhibit

*Correspondence to: Ángela Sastre-Santos, e-mail: asastre@umh.es, telephone: +34 9666658408

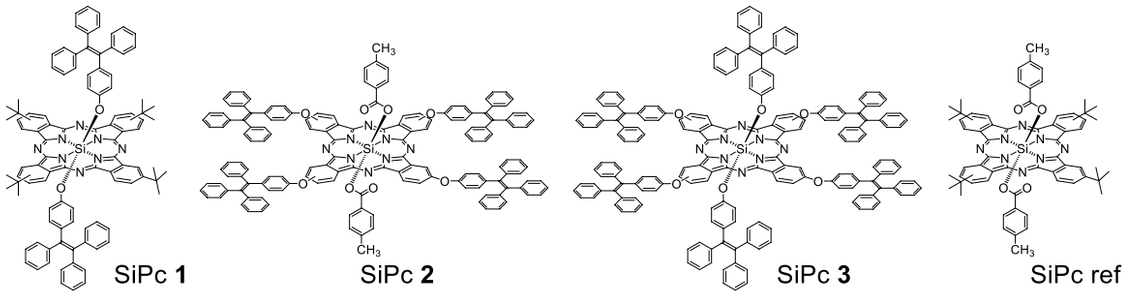

Chart 1. Chemical structure of SiPc **1**, SiPc **2**, SiPc **3** and SiPc ref.

enhanced fluorescence in the aggregated state compared to their monomeric form [8, 9]. AIEgens typically possess rotatable bonds, such as hexaphenylsilole (HPS) [10], triphenylamine (TPA) [11], or tetraphenylethene (TPE) [12]. The AIE effect occurs because, in solution, the fluorescence is quenched by rotational and vibrational energy dissipation, but when aggregation occurs, these motions are restricted, resulting in increased emission intensity. Since the initial discovery of AIE, AIEgens have been incorporated into various chromophores, including porphyrins [13], subphthalocyanines [14], and phthalocyanines [15, 16], to transform them from ACQ-type to AIE photosensitizers, enhancing their applicability in photovoltaics, PDT, or near-infrared (NIR) fluorescent bioimaging [17].

Here we present the synthesis, characterization, and evaluation of the photophysical properties and singlet oxygen generation of a series of silicon phthalocyanine compounds, SiPc **1**, SiPc **2** and SiPc **3** (Chart 1), bearing tetraphenylethene (TPE) units, an AIEgen, located at both axial and peripheral positions, to investigate the influence of TPE positioning on photophysical properties, singlet oxygen generation, and aggregation-induced emission characteristics.

EXPERIMENTAL

General methods

All chemicals were reagent grade, purchased from commercial sources, and were used as received unless otherwise specified. Microwave reactions were carried out in a CEM microwave reactor using the Discover SP model. Column chromatography was performed on SiO_2 (40–63 mm). TLC plates coated with SiO_2 60F254 were visualized under UV light. NMR spectra were acquired on a Bruker 400 MHz spectrometer. UV/Vis spectra were recorded on a Perkin Elmer LAMBDA 365 UV-WinLab spectrophotometer. Fluorescence spectra were recorded on a Horiba Scientific FluoroMax-4 TCSPC spectrofluorometer employing quartz cuvettes with 1 cm path length. High-resolution mass spectra were obtained from a Bruker Reflex II matrix-assisted laser desorption/ionization time-of-flight (MALDI-TOF) spectrometer using dithranol as matrix.

Synthesis

Preparation of (^{t}Bu)$_4$SiPc(TPE)$_2$ (SiPc 1)

In a 10 mL microwave tube, (^{t}Bu)$_4$SiPcCl$_2$ **6** (50 mg, 0.060 mmol), 4-(1,2,2-Triphenylvinyl)phenol (104 mg, 0.298 mmol) were dissolved in dry toluene (0.75 mL) and 1-methyl-2-pyrrolidone (NMP, 0.25 mL). The contents were stirred and microwave-irradiated to a set temperature of 160 °C for 60 min. The crude reaction mixture was precipitated in methanol, filtered and purified by column chromatography (SiO_2, $CHCl_3$). This yielded 8 mg (12%) of pure compound as a green solid. ^{1}H NMR (400 MHz, $CDCl_3$, 25 °C): δ 9.63–9.57 (m, 4H, H-Pc), 9.57–9.45 (m, 4H, H-Pc), 8.46–8.40 (m, 4H, H-Pc), 6.97–6.81 (m, 12H, H-TPE), 6.66–6.49 (m, 10H, H-TPE), 6.28–6.20 (m, 8H, H-TPE), 5.26 (d, J = 8.6 Hz, 4H, H-TPE), 2.23 (d, J = 8.6 Hz, 4H, H-TPE) and 1.83 (m, 36H, 12xCH_3). UV/Vis (THF): λ_{max} (log ε) = 339 (4.94), 355 (4.94), 616 (4.58), 656 (4.51), 686 (5.33). HR-MS (MALDI-TOF, dithranol) $C_{100}H_{86}N_8O_2Si$: m/z for $[M]^-$ calcd. 1458.6592, found 1458.6651.

Preparation of (TPE)$_4$-SiPc(Tol)$_2$ (SiPc 2)

In a 10 mL microwave tube, (TPE)$_4$SiPcCl$_2$ **7** (50 mg, 0.025 mmol), 4-methylbenzoic acid (17 mg, 0.125 mmol) were dissolved in dry toluene (0.75 mL) and 1-methyl-2-pyrrolidone (NMP, 0.25 mL). The contents were stirred and microwave-irradiated to a set temperature of 160°C for 60 min. The crude reaction mixture was precipitated in methanol, filtered and purified by column chromatography (SiO_2, $CHCl_3$). This yielded 22 mg (40%) of pure compound as a green solid. ^{1}H NMR (400 MHz, $CDCl_3$, 25 °C): δ 9.58–9.50 (m, 4H, H-Pc), 9.10–9.01 (m, 4H, H-Pc), 8.00–7.90 (m, 4H, H-Pc), 7.33–7.06 (m, 76H, H-TPE), 6.06 (d, J = 8.1 Hz, 4H, H-Ar), 5.04 (d, J = 8.1 Hz, 4H, H-Ar) and 1.71 (s, 6H, 2xCH_3). UV/Vis (THF): λ_{max} (log ε) = 347 (5.02), 625 (4.63), 695 (5.28). HR-MS (MALDI-TOF, dithranol) $C_{152}H_{102}N_8O_8Si$: m/z for $[M]^+$ calcd. 2194.7492, found 2194.7922.

Preparation of (TPE)$_4$-SiPc(TPE)$_2$ (SiPc 3)

In a 10 mL microwave tube, (TPE)$_4$SiPcCl$_2$ **7** (50 mg, 0.025 mmol), 4-(1,2,2-Triphenylvinyl)phenol (44 mg, 0.125 mmol) were dissolved in dry toluene (0.75 mL) and 1-methyl-2-pyrrolidone (NMP, 0.25 mL). The contents were stirred and microwave-irradiated to a set temperature of 160 °C for 60 min. The crude reaction mixture was precipitated in methanol, filtered and purified by column chromatography (SiO_2, $CHCl_3$). This yielded 8 mg (12%) of pure compound as a green solid. ^{1}H NMR (400 MHz, $CDCl_3$, 25 °C): δ 9.51–9.40 (m, 4H, H-Pc), 9.02–8.95 (m, 4H, H-Pc), 7.99–7.88 (m, 4H, H-Pc), 7.40–7.04 (m, 76H, H-TPE periphery), 6.97-6.82 (m, 12H, H-TPE axial), 6.59-6.53 (m, 10H, H-TPE axial), 6.32-6.21 (m, 8H, H-TPE axial), 5.30 (d, J=8.7 Hz, 4H, H-TPE axial) and 2.23 (d, J=8.7 Hz, 4H, H-TPE axial). UV/Vis (THF): λ_{max} (log ε)=339 (4.92), 621 (4.40), 693 (5.21). HR-MS (MALDI-TOF, dithranol): $C_{188}H_{126}N_8O_6Si$: m/z for $[M]^-$ calcd. 2618.9414, found 2618.8064.

Preparation of TPE-phtalonitrile 4

In a 50 mL round-bottom flask, 4-(1,2,2-triphenylvinyl)phenol (1.00 g, 2.87 mmol) and 4-nitrophthalonitrile (0.50 g, 2.89 mmol) were dissolved in 20 mL of dry DMF. K_2CO_3 (0.60 g, 4.34 mmol) was added in batches over 1.5 hours. The mixture was then stirred at room temperature for 48 hours. The reaction mixture was poured into 50 mL of ice-cold water upon completion. The resulting precipitate was filtered and washed several times with water. The solid was dried and then recrystallized from ethanol, yielding 1.12 g (82%) of pure compound as a milky powder. ^{1}H NMR (400 MHz, DMSO-d^6, 25 °C): δ (ppm): 8.12 (d, J=8.8 Hz, 1H, Ar-H), 7.61 (d, J=2.6 Hz, 1H, Ar-H), 7.30 (dd, J=8.8 Hz and J=2.6Hz, 1H, Ar-H), 7.22–6.93 (m, 19H, H-TPE). ^{13}C NMR (100 MHz, DMSO-d^6, 25 °C):161.0, 152.1, 143.0, 142.8, 142.6, 141.2, 140.9, 139.6, 136.3, 132.8, 130.7, 130.6, 130.6, 127.9, 127.9, 126.7, 126.7, 122.4, 121.9, 119.8, 116.7, 115.9, 115.4, 108.2. HR-MS (MALDI-TOF, dithranol) $C_{34}H_{22}N_2O$: m/z for $[M]^+$ calcd. 474.1729, found 474.1731.

Preparation of TPE-diiminoisoindoline 5

In a 250 mL round-bottom flask, TPE-phthalonitrile **4** (0.50 g, 1.05 mmol) and MeONa (0.14 g, 2.59 mmol) were dissolved in 100 mL of MeOH. The mixture was stirred at room temperature for 1 hour while purging with NH_3 gas, and the solution was then brought to reflux for 10 hours. The reaction completion was monitored by thin-layer chromatography. Afterward, the solvent was evaporated, and the resulting powder was recrystallized from ethanol, yielding 0.51 g (99%) of greenish powder, which was used in the subsequent steps without further purification. ^{1}H NMR (400 MHz, DMSO-d_6, 25 °C): δ (ppm): 7.82 (d, J=8.2 Hz, 1H, Ar-H), 7.82 (d, J=8.2 Hz, 1H, Ar-H), 7.30 (dd, J=8.2 Hz and J=2.2 Hz, 1H, Ar-H), 7.22–6.93 (m, 19H, H-TPE). HR-MS (MALDI-TOF, dithranol) $C_{34}H_{25}N_3O$: m/z for $[M+H]^+$ calcd. 492.1957, found 492.1960.

Preparation of (TPE)$_4$-SiPcCl$_2$ 6

In a 50 mL round-bottom flask, TPE-diiminoisoindoline **5** (0.50 g, 1.02 mmol) was dissolved in 5 mL of dry quinoline under an argon atmosphere for 10 minutes in the dark. Then, 0.5 mL of $SiCl_4$ was slowly added under vigorous stirring. The mixture was brought to reflux temperature and maintained for 1 hour. Upon completion, the crude product was cooled to room temperature, then precipitated in hot acetone, filtered under vacuum, and carefully washed. This process yielded 0.49 g (96%) of (TPE)$_4$-SiPcCl$_2$ **6**. The product was stored in the dark under argon for use without further purification. UV/Vis (THF): λ_{max}/nm 375, 634, 707.

Singlet oxygen quantum yield determination

Singlet oxygen quantum yield (Φ_Δ) determinations were carried out in a 3 mL portion of solutions containing the singlet oxygen quencher irradiated in the Q band region with the photo-irradiation set-up described in the reference [18]. For singlet oxygen measurements, 1,3-diphenylisobenzofuran (DPBF) was used as an oxygen scavenger and its degradation at 417 nm was monitored by UV–Vis spectroscopy. The solutions of photosensitizers containing DPBF (~3x10^{-5} M) were prepared in the dark and irradiated in the Q band region.

RESULTS AND DISCUSSION

Synthesis and characterization

The synthesis of SiPc **1** is described in Scheme 1. It was prepared with a 12% yield by nucleophilic substitution of the two axial chlorine atoms of freshly prepared (^{t}Bu)$_4$SiPcCl$_2$ **6**, using a 5-equivalent quantity of 4-(1,2,2-triphenylvinyl)phenol (TPE-OH). The reaction was carried out under microwave radiation for 1 hour in

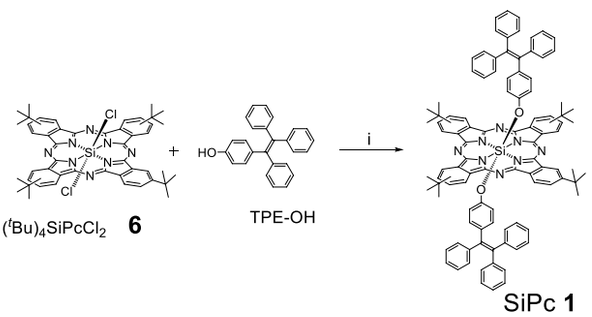

Scheme 1. Synthesis of SiPc **1**. Reagents and conditions: (i) Tol/NMP 3:1 v/v, Ar, MW:160 °C/200 W/ 1h, 12 %.

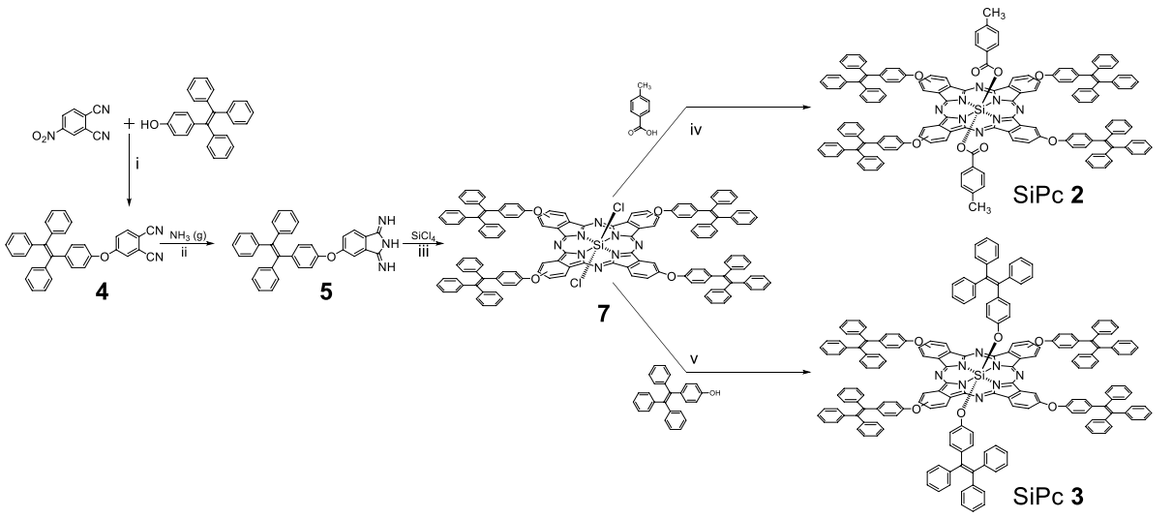

Scheme 2. Synthesis of SiPc **2** and SiPc **3**. Reagents and conditions: (i) anhydrous K_2CO_3, DMF, RT, Ar, 48 h. 82%; (ii) MeONa/MeOH, 65 °C, 10 h, 99%; (iii) dry quinoline, reflux, dark, Ar, 1 h, 99%, (iv) Tol/NMP 3:1 v/v, Ar, MW:160 °C/200 W/ 1h, 40 %, (v) Tol/NMP 3:1 v/v, Ar, MW:160 °C/200 W/ 1h, 12 %.

a 3:1 mixture of toluene and *N*-methyl-2-pyrrolidone, the latter added to enhance microwave energy absorption [19].

The synthesis of SiPcs **2** and **3** is detailed in Scheme 2. Starting from 4-nitrophthalonitrile, an S_NAr reaction with TPE-OH, adapted from an already reported procedure [16], yielded 4-(4-(1,2,2-triphenylvinyl)phenoxy)phthalonitrile **4**. This intermediate was then converted into the more reactive 4-(4-(1,2,2-triphenylvinyl)phenoxy) isoindoline-1,3-diimine **5** by treatment with ammonia in refluxing methanol and a catalytic amount of MeONa, following a previously described method [20]. A subsequent cyclotetramerization reaction of **5** was performed in dry quinoline with $SiCl_4$ at reflux temperature for 1 hour, avoiding direct light exposure. After rapid isolation, $(TPE)_4SiPcCl_2$ **7** was obtained as a green solid and used in the final steps without further purification. It is noteworthy that the nucleophilic displacement of axial chlorine atoms, using conditions similar to those for SiPc **1**, is more efficient when *p*-methylbenzoic acid is used for axial functionalization, yielding SiPc **2** with a 40% yield, compared to a 12% yield for SiPc **3** when TPE-OH is used, similar to that obtained for SiPc **1**. This difference is likely due to the steric hindrance of TPE-OH, making it more challenging to approach the inner silicon atom than *p*-methylbenzoic acid.

NMR and mass spectroscopy characterization

All new compounds were characterized by ^{1}H-NMR spectroscopy and HR-MALDI-TOF mass spectrometry. Figure 1 compares ^{1}H-NMR spectra of SiPc **ref**, SiPc **1**, SiPc **2**, and SiPc **3**. The axial substitution of these compounds effectively moderated aggregation phenomena in $CDCl_3$, resulting in high-resolution ^{1}H-NMR spectra that facilitated signal assignments. Moreover, comparing the ^{1}H-NMR signals of the previously assigned SiPc

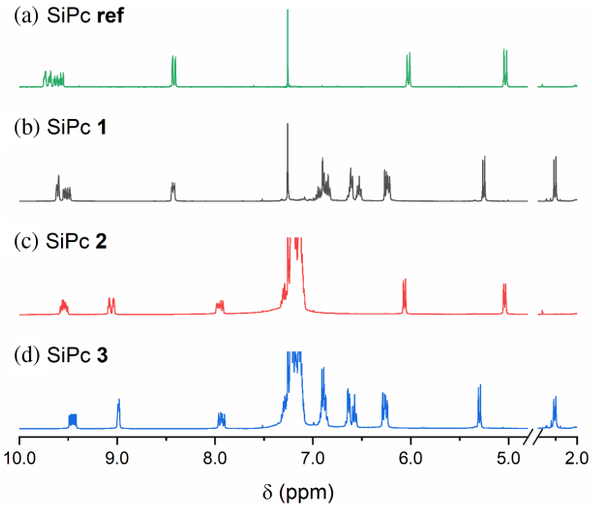

Fig. 1. ^{1}H-NMR spectra, registered in $CDCl_3$ at RT of (a) SiPc **ref**, (b) SiPc **1**, (c) SiPc **2** and (d) SiPc **3**.

ref [21] (Fig. 1a) enabled us to unambiguously identify the peaks in the spectra of the new SiPc compounds. In the ^{1}H-NMR spectrum of SiPc **1** (Fig. 1b), the phthalocyanine ring hydrogens appear as multiplets at 9.61, 9.51 and 8.43 ppm, each integrating for four hydrogens. The hydrogens of TPE axial substituents appear as multiplets at 6.90, 6.57, and 6.25 ppm, integrating for 12, 10, and 8 hydrogens, respectively, and were assigned to those of the distant phenyl units. Two coupled doublets at 5.25 and 2.23 ppm, each integrating for four protons, were transferred to the hydrogens of phenoxy axial groups directly bonded to the silicon center, and are visibly downfield shifted, an effect which is attributable to the SiPc core ring current. Similarly, SiPc **2** (Fig. 1c) displays phthalocyanine ring proton signals at 9.54, 9.06, and

7.95 ppm, each integrating for four hydrogens. Hydrogens of peripheral TPE groups show as a broad multiplet centered at 7.19 ppm, integrating for 76 hydrogens. In contrast, *p*-methylbenzoate axial groups appear as two coupled doublets, at 6.06 and 5.04 ppm, each integrating for four aromatic protons. Finally, SiPc **3**, with TPE units in either axial and peripheral positions, exhibits ^{1}H-NMR spectral features consistent with those observed in SiPc **1** and SiPc **2** (Fig. 1d).

HR-MS-MALDI-TOF assays revealed peaks corresponding to the molecular ion of each analyzed molecule. Peaks corresponding to the fragmentation of one or two axial groups are a common feature in SiPc mass spectra (see SI).

Photophysical properties

UV-vis and fluorescence spectra, and photostimulated singlet oxygen generation

Figure 2 shows the UV-vis absorption spectra of SiPc **1**, SiPc **2**, and SiPc **3**, acquired in THF at room temperature, together with that of SiPc ref, a peripherally *tert*-butyl-substituted SiPc with two axial *p*-methylbenzoate ligands (Chart 1), synthesized according to established procedures [21] and employed as a comparative reference. The spectra exhibit well-defined profiles, consistent with the observed reduction in aggregation propensity attributed to axial substitution, and display characteristic phthalocyanine absorption features, including a B-band within the 350–380 nm region and an intense Q-band around 685–700 nm. SiPc **2** and SiPc **3**, bearing peripheral TPE units, display a broadened Q-band, suggesting a weak aggregation tendency potentially arising from intermolecular interactions of the peripheral TPE moieties. This effect, however, remains significantly attenuated by the axial substitution strategy. Variations in the Q-band maximum wavelength are attributed to the enhanced electron-donating character of the peripheral TPE substituents relative to *tert*-butyl groups and the specific axial ligands. A blue shift of 3–5 nm is observed for SiPc **1** and SiPc **3** when compared to SiPc ref and SiPc **2**, respectively, indicating the influence of axial ligand structure on the electronic transitions of the SiPc core. Furthermore, the presence of TPE units is evidenced by an increased absorbance below 350 nm, corresponding to the absorption maxima of the TPE-OH and TPE-phthalonitrile **4** precursor (see SI). This spectral feature confirms the successful incorporation of TPE moieties into the SiPc structures. These bands are not attributable to residual starting materials or impurities, as confirmed with the NMR analysis of SiPcs.

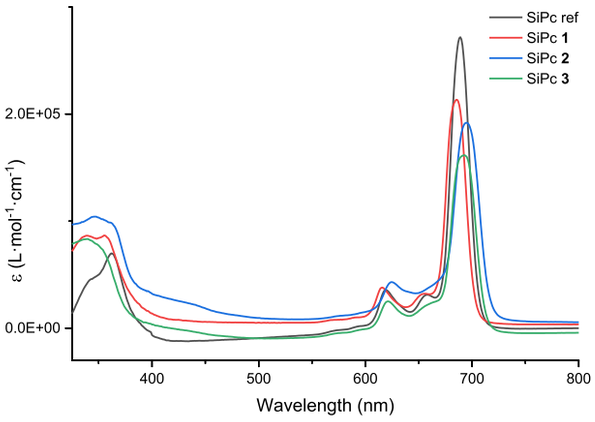

Fig. 2. UV-vis spectra, registered in THF (10^{-6} M) at RT, of SiPc ref, SiPc **1**, SiPc **2**, and SiPc **3**.

Figure 3 presents the fluorescence emission spectra of SiPc **1**, SiPc **2**, SiPc **3**, and SiPc ref, obtained from 10^{-6} M THF solutions at room temperature. Upon selective excitation at the first vibronic band of the Q-band absorption, all compounds exhibit similar spectral profiles, characterized by emission maxima within the 675–700 nm range and a shoulder at 750–790 nm. A notable observation is the decreased fluorescence intensity of SiPc **1** and SiPc **3**, axially substituted with TPE ligands, compared to SiPc ref and SiPc **2**.

The fluorescence quantum yields (Φ_F) of SiPc **1**, SiPc **2**, and SiPc **3** are listed in Table 1 and have been determined using a modified experimental protocol [22] in THF at room temperature, utilizing unsubstituted zinc phthalocyanine (ZnPc) as a standard ($\Phi_{F(std)}=0.23$) and applying equation (1), where F represents the integrated emission area, A denotes the absorbance, and n signifies the solvent refractive index.

$$\Phi_F = \Phi_{F(std)} \frac{F_{sample}}{F_{std}} \frac{A_{std}}{A_{sample}} \frac{n^2_{sample}}{n^2_{std}}. \quad (1)$$

The data reveal a significant decrease in Φ_F values for the axially TPE-substituted SiPc compounds, SiPc **1** and SiPc **3**. This reduction in emission intensity can be attributed to an increased conformational flexibility facilitated

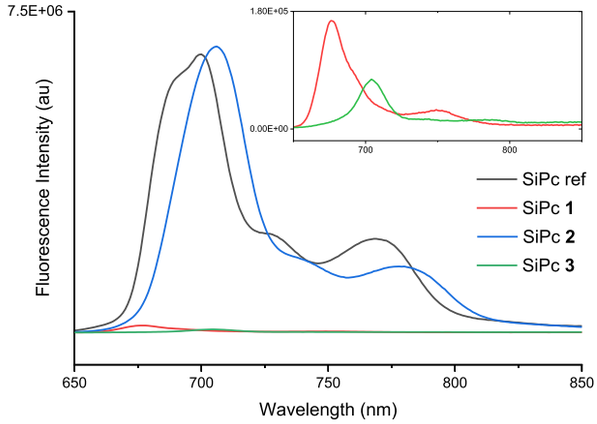

Fig. 3. Fluorescence emission spectra, registered in THF (10^{-6} M) at RT, of SiPc ref ($\lambda_{exc}=621$ nm), SiPc **1** ($\lambda_{exc}=615$ nm), SiPc **2** ($\lambda_{exc}=615$ nm) and SiPc **3** ($\lambda_{exc}=620$ nm). Inset: enlarged view of SiPc **1** and SiPc **3** fluorescent emission spectra.

Table 1. Photophysical properties and $^1O_2$ generation of SiPc **1**, SiPc **2** and SiPc **3**.

Compound	Absorption	Emission			$^1O_2$
	λ_{max} (nm)	λ_{exc} (nm)	λ_{em} (nm)	Φ_F	Φ_Δ
SiPc ref	689	621	700	0.351	0.21
SiPc **1**	685	615	675	0.007	0.09
SiPc **2**	695	615	706	0.297	0.37
SiPc **3**	692	620	705	0.004	0.08

by the axial TPE substituents, which increases the possibility of dissipating excited energy through intramolecular rotation [23].

The singlet oxygen quantum yield (Φ_Δ), an essential parameter for assessing photosensitizer efficiency in generating singlet oxygen ($^1O_2$), was determined for each SiPc using a spectroscopic method [24]. This method involves monitoring the photobleaching of diphenylisobenzofuran (DPBF), a singlet oxygen scavenger, in THF, utilizing ZnPc as a standard (Φ_Δ=0.53) [25]. The Φ_Δ values, presented in Table 1, were calculated using equation (2).

$$\Phi_\Delta = \Phi_{\Delta(std)} \frac{m_{sample}}{m_{std}} \quad (2)$$

where m represents the slope of the linear regression of change in absorbance of DPBF (at 417 nm) *vs* irradiation time, and shows the influence of axial TPE substituents in the photostimulated singlet oxygen generation (See SI).

Aggregation-induced emission properties

The synthesized compounds' aggregation-induced emission (AIE) characteristics were evaluated through fluorescence emission measurements in THF/water mixtures of varying water fractions (fw). A 10^{-6} M THF solution of TPE-phthalonitrile **4**, upon excitation at 270 nm (TPE unit absorption), exhibited an emission band centered at 370 nm. The emission intensity increased with incremental water addition, reaching the maximum at 30–40%, followed by a decrease, indicating AIE characteristics of the TPE-phthalonitrile precursor (see SI). In contrast, under identical excitation and water addition conditions, 10^{-6} M THF solutions of SiPc **1**, SiPc **2**, and SiPc **3** did not demonstrate AIE attributable to TPE unit aggregation. Instead, significant variations in the phthalocyanine unit emission profiles were observed. A consistent decrease in fluorescence maximum intensity is observed across all compounds with increasing water content, with the maximum effect observed at water fractions around 40–60% (Fig. 4). This phenomenon aligns with the established aggregation-caused quenching (ACQ) effect, due to the limited solubility and hydrophilicity of the SiPc molecules. While ACQ is consistently observed, a divergent trend emerges for compounds without TPE units in peripheral positions, particularly SiPc **1**. SiPc ref (Fig. 4a) exhibits a significant redshift

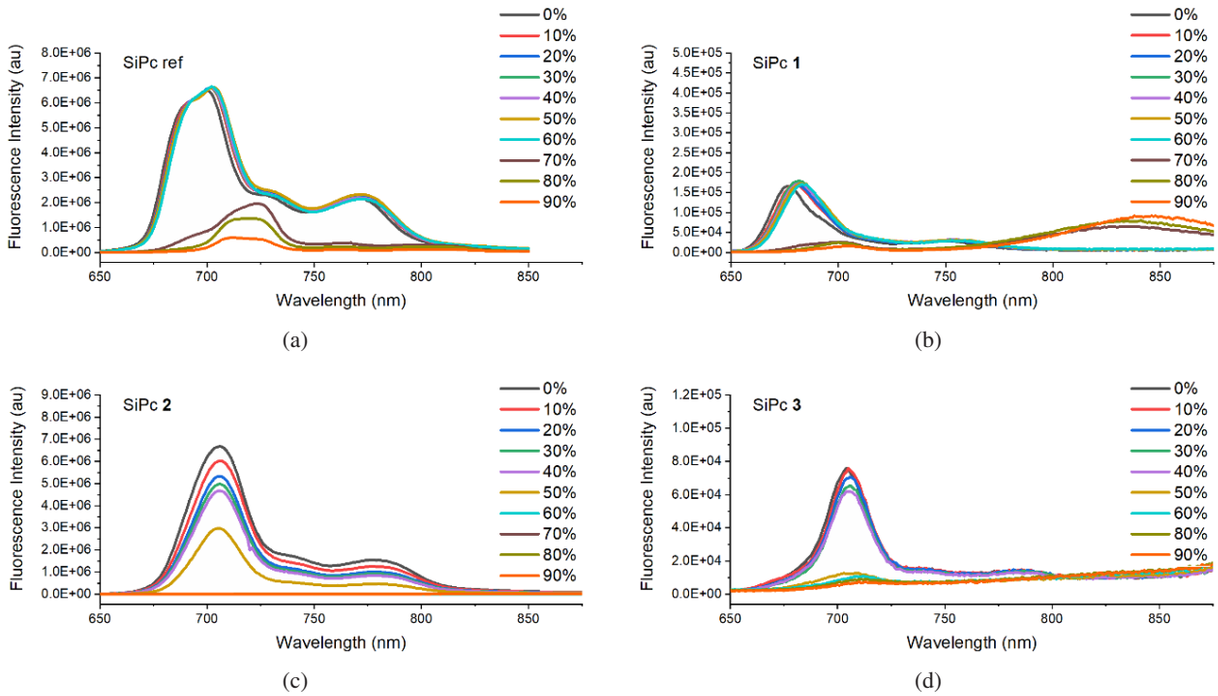

Fig. 4. Fluorescence emission spectra, registered in THF (10^{-6} M) at RT, of (a) SiPc ref (λ_{exc}=621 nm), (b) SiPc **1** (λ_{exc}=615 nm), (c) SiPc **2** (λ_{exc}=615 nm) and (d) SiPc **3** (λ_{exc}=620 nm), with different water contents.

in the fluorescence maximum wavelength from 700 nm to 725 nm at fw 70%, followed by gradual quenching up to fw 90%. In contrast, SiPc **1** (Fig. 4b), featuring axial TPE substituents, displays a similar redshift, accompanied by the emergence of a novel emission band centered at 833 nm at fw 70%, which is gradually redshifted and increased in intensity as the water content rises to 90% (847 nm). This distinct behavior suggests the formation, induced by the axial TPE ligands, of a novel SiPc-based emissive species, likely *J*-aggregates, exhibiting inherent AIE properties [26]. This effect is not observed in SiPc **3** (Fig. 4d), bearing TPE in axial positions and four peripheral TPE units. These seem to interfere significantly with forming the already commented SiPc-based AIE aggregates.

CONCLUSION

Three novel silicon phthalocyanine derivatives, peripherally and axially substituted with tetraphenylethylene (TPE) units, have been synthesized and characterized. Photophysical and aggregation-induced emission (AIE) properties revealed distinct behaviors among the synthesized compounds. SiPc **1**, axially substituted with TPE, exhibited decreased fluorescence quantum yields, singlet oxygen generation, and the formation of novel emissive species in the near-infrared region (700–900 nm), demonstrating AIE upon water addition. On the other hand, SiPc **2**, featuring four peripheral TPE units and no axial TPE units, displayed enhanced fluorescence quantum yield and singlet oxygen generation, without AIE occurrence. SiPc **3**, incorporating TPE units in axial and peripheral positions, showed diminished fluorescence quantum yields, reduced singlet oxygen generation, and no AIE. These observations indicate that strategic TPE substitution on silicon phthalocyanines allows for the modulation of both photodynamic activity and AIE properties and suggest that TPE-substituted SiPcs can be designed to combine photodynamic activity with AIE, which could be beneficial for applications in image-guided phototherapy and other biomedical applications. Further studies should optimize the balance between AIE and singlet oxygen generation to maximize their therapeutic potential.

Acknowledgments

We want to express our gratitude to the European Regional Development Fund "A Way to Make Europe," the Spanish Ministerio de Ciencia e Innovación/Agencia Estatal de Investigación (PID2020-117855 RB-I00 to Á.S.-S.), and the Generalitat Valenciana (CIPROM/2021/059 and MFA/2022/028 to Á. S.-S.) for their funding. The MFA projects are part of the Advanced Materials programme supported by MCIN, with funding from the European Union's NextGenerationEU (PRTR-C17.I1) and the Generalitat Valenciana.

Supporting information

Additional data are given in the supplementary material. This material is available free of charge *via* the Internet at http://www.worldscientific.com/doi/suppl/10.1142/S1088424625500622

REFERENCES

1. De La Torre G, Claessens CG and Torres T. *Chem. Commun.* 2007; 2000–2015.
2. Ragoussi M and Torres T. *Chem. — Asian J.* 2014; **9**: 2676–2707.
3. Dougherty TJ, Gomer CJ, Henderson BW, Jori G, Kessel D, Korbelik M, Moan J and Peng Q. *JNCI, J. Natl. Cancer Inst.* 1998; **90**: 889–905.
4. Lo P-C, Rodríguez-Morgade MS, Pandey RK, Ng DKP, Torres T and Dumoulin F. *Chem. Soc. Rev.* 2020; **49**: 1041–1056.
5. Mitra K and Hartman MCT. *Org. Biomol. Chem.* 2021; **19**: 1168–1190.
6. Saha P, Das S, Indurthi HK and Sharma DK. *Dyes Pigm.* 2022; **206**: 110608.
7. Dumoulin F, Durmuş M, Ahsen V and Nyokong T. *Coord. Chem. Rev.* 2010; **254**: 2792–2847.
8. Mei J, Hong Y, Lam JWY, Qin A, Tang Y and Tang BZ. *Adv. Mater.* 2014; **26**: 5429–5479.
9. Mei J, Leung NLC, Kwok RTK, Lam JWY and Tang BZ. *Chem. Rev.* 2015; **115**: 11718–11940.
10. Zhang T, Jiang Y, Niu Y, Wang D, Peng Q and Shuai Z. *J. Phys. Chem. A* 2014; **118**: 9094–9104.
11. Yang Z, Yin W, Zhang S, Shah I, Zhang B, Zhang S, Li Z, Lei Z and Ma H. *ACS Appl. Bio Mater.* 2020; **3**: 1187–1196.
12. Yang Z, Qin W, Leung NLC, Arseneault M, Lam JWY, Liang G, Sung HHY, Williams ID and Tang BZ. *J. Mater. Chem. C* 2016; **4**: 99–107.
13. Bodedla GB, Zhu X and Wong W. *Aggregate* 2023; **4**: e330.
14. (a) Ding W, Yan L, Cao F and Luo Q. *Tetrahedron Lett.* 2021; **73**: 153096; (b) Furuyama T, Shitanda S, Fukumura T. and Kobayashi N. *J. Porphyrins Phthalocyanines* 2023; **27**: 1156.
15. Liu G, Guo Q, Huang B, Guan X, Ye Q, Zhuang X and Peng Y. *Inorg. Chem. Commun.* 2022; **141**: 109490.
16. Gümüşgöz Çelik G, Tunç G, Lafzi F, Saracoglu N, Seçkin Arslan B, Nebioğlu M, Şişman İ and Gürek AG *J. Photochem. Photobiol. A: Chem.* 2023; **444**: 114962.
17. Zhu W, Huang L, Wu C, Liu L and Li H. *Luminescence* 2024; **39**: e4655.
18. Ogunsipe A and Nyokong T. *J. Photochem. Photobiol. A: Chem.* 2005; **173**: 211–220.
19. Kappe CO. *Angew. Chem., Int. Ed.* 2004; **43**: 6250–6284.

20. Sastre Á, Del Rey B and Torres T. *J. Org. Chem.* 1996; **61**: 8591–8597.
21. Martín-Gomis L, Ohkubo K, Fernández-Lázaro F, Fukuzumi S and Sastre-Santos Á. *Org. Lett.* 2007; **9**: 3441–3444.
22. Ogunsipe A, Maree D and Nyokong T. *J. Mol. Struct.* 2003; **650**: 131–140.
23. Ding W, Yan L, Cao F and Luo Q. *Tetrahedron Lett.* 2021; **73**: 153096.
24. Blacha-Grzechnik A, Drewniak A, Walczak KZ, Szindler M and Ledwon P. *J. Photochem. Photobiol. A: Chem.* 2020; **388**: 112161.
25. Ma D, Chen X, Wang Y, Guo Q, Ye Q, Guo R, Xiao S, Ye Q, Huang Y and Peng Y. *J. Lumin.* 2019; **207**: 597–601.
26. Doane T, Chomas A, Srinivasan S and Burda C. *Chem. — A Eur. J.* 2014; **20**: 8030–8039.